TITLE

Amazon forest response to CO_2 fertilization dependent on plant phosphorus acquisition

AUTHORS AFFILITATIONS

Katrin Fleischer*, *Land Surface–Atmosphere Interactions, Technical University of Munich, Germany*

Anja Rammig, *Land Surface–Atmosphere Interactions, Technical University of Munich, Germany*

Martin G. De Kauwe[1,2], [1]*Climate Change Research Centre, University of New South Wales, Sydney, NSW 2052, Australia;* [2]*ARC Centre of Excellence for Climate Extremes, Sydney, NSW 2052, Australia*

Anthony P. Walker, *Environmental Sciences Division and Climate Change Science Institute, Oak Ridge National Laboratory, Oak Ridge, TN, USA*

Tomas F. Domingues, *FFCLRP, Department of Biology, University of São Paulo, Brazil*

Lucia Fuchslueger[1,2], [1]*National Institute of Amazonian Research (INPA), Brazil;* [2]*University of Antwerp, Belgium*

Sabrina Garcia, *National Institute of Amazonian Research (INPA), Brazil*

Daniel S. Goll[1,2], [1]*Laboratoire des Sciences du Climat et de l'Environnement, LSCE/IPSL, CEA–CNRS–UVSQ, France;* [2]*Lehrstuhl für Physische Geographie mit Schwerpunkt Klimaforschung, Universität Augsburg, Alter Postweg 118, D-86135 Augsburg, Germany*

Adriana Grandis, *University of São Paulo, Brazil*

Mingkai Jiang, *Hawkesbury Institute for the Environment, Western Sydney University, Australia*

Vanessa Haverd, *CSIRO Oceans and Atmosphere, Canberra, 2601, Australia*

Florian Hofhansl, *International Institute for Applied Systems Analysis, Schlossplatz 1, A-2361 Laxenburg, Austria*

Jennifer A. Holm, *Lawrence Berkeley National Laboratory, Berkeley, California, United States*

Bart Kruijt, *Alterra Wageningen, The Netherlands*

Felix Leung[1,2], [1]*College of Life and Environmental Sciences, University of Exeter, EX4 4QE, UK;* [2]*Institute of Environment, Energy and Sustainability, The Chinese University of Hong Kong, Hong Kong*

Belinda E. Medlyn, *Hawkesbury Institute for the Environment, Western Sydney University, Australia*

Lina M. Mercado[1,2], *[1]College of Life and Environmental Sciences, University of Exeter, EX4 4QE, UK; [2]Centre for Ecology and Hydrology, Wallingford, OX10 8BB, UK*

Richard J. Norby, *Environmental Sciences Division and Climate Change Science Institute, Oak Ridge National Laboratory, Oak Ridge, TN, USA*

Bernard Pak, *CSIRO Oceans and Atmosphere, Aspendale Victoria 3195, Australia*

Carlos A. Quesada, *National Institute of Amazonian Research (INPA), Brazil*

Celso von Randow, *National Institute for Space Research (INPE), Brazil*

Karst J. Schaap, *National Institute of Amazonian Research (INPA), Brazil*

Oscar J. Valverde-Barrantes, *International Center of Tropical Botany, Florida International University, United States*

Ying-Ping Wang, *CSIRO Oceans and Atmosphere, Aspendale Victoria 3195, Australia*

Xiaojuan Yang, *Environmental Sciences Division and Climate Change Science Institute, Oak Ridge National Laboratory, Oak Ridge, TN, USA*

Sönke Zaehle, *Max-Planck Institute for Biogeochemistry, Germany*

Qing Zhu, *Lawrence Berkeley National Laboratory, Berkeley, California, United States*

David M. Lapola, *Center for Meteorological and Climatic Research Applied to Agriculture, University of Campinas, Brazil*

*corresponding author

MAIN TEXT

Global terrestrial models currently predict that the Amazon rainforest will continue to act as a carbon sink in the future primarily due to the rising atmospheric carbon dioxide (CO_2) concentration. Soil phosphorus impoverishment in parts of the Amazon basin largely controls its functioning, but the role of phosphorus availability has not been considered in global model ensembles, e.g., during the 5th Climate Model Intercomparison Project (CMIP5). Here, we simulate the planned free-air CO_2 enrichment experiment AmazonFACE with an ensemble of 14 terrestrial ecosystem models. We show that phosphorus availability reduces the projected CO_2-induced biomass carbon growth by about 50% to 79 ± 63 g C m^{-2} yr^{-1} over 15 years compared to estimates from carbon and carbon-nitrogen models. Our results suggest that the region's resilience to climate change may be much less than previously assumed. Variation in the biomass carbon response among the phosphorus-enabled models is considerable, ranging from 5 to 140 g C m^{-2} yr^{-1}, due to contrasting plant phosphorus use and acquisition strategies considered among the models. The Amazon forest response will thus depend on the interactions and relative contributions of the phosphorus acquisition and use strategies across individuals, and to what extent these processes can be upregulated under eCO_2.

The intact Amazon rainforest acts as a substantial carbon (C) sink, completely offsetting carbon dioxide (CO_2) emissions from fossil fuel combustion and land use change in the Amazon region[1,2]. Increasing atmospheric CO_2 concentrations from anthropogenic activity may be the primary factor for the current Amazon net C sink[1,3], via so-called CO_2 fertilization (an increase in photosynthetic C uptake by plants under higher CO_2), which is projected to continue into the future by global models[4–6]. The CO_2 fertilization effect has been observed experimentally in field experiments that were conducted predominantly in the temperate zone.

In these experiments, the eCO_2 induced increase in C uptake was generally low when other factors, such as soil nitrogen (N), were limiting[7–9]. To date, whole-ecosystem-scale experiments, i.e., free-air CO_2 enrichment (FACE) have never been conducted in the tropics[10,11].

Over large parts of the Amazon and the tropics worldwide, phosphorus (P), not N, is assumed to be the key limiting nutrient, as most P has been lost or occluded from plant uptake during millions of years of soil pedogenesis[12,13]. Forests growing on these highly weathered old soils may nonetheless be highly productive due to the evolution of multiple strategies for P acquisition and use, enabling tight cycling of P between plants and soils[14,15]. Despite this knowledge, quantifying the control of P on plant physiology, growth, and plant-soil interactions in global models, and hence its role in the forests' response to eCO_2, remains challenging[16,17]. This challenge is exacerbated by the scarcity of observations and distinctive species responses in hyperdiverse tropical forests[18].

Predicted nutrient feedbacks to eCO_2 at the AmazonFACE site

Here, we study the potential interactions between eCO_2 and nutrient (N and P) feedbacks in a mature Amazonian rainforest by simulating the planned AmazonFACE experiment (+200 ppm; https://amazonface.inpa.gov.br/) with an ensemble of ecosystem models (n = 14, Extended Data Table 3), including three C, five carbon-nitrogen (CN), and six carbon-nitrogen-phosphorus (CNP) models[19–24]. The AmazonFACE experiment is located in a well-studied, highly productive tropical forest in Central Amazonia[25,26], growing on a strongly weathered *terra firme* Ferralsol. This ecosystem represents the low end of the plant-available P spectrum in the Amazon, consistent with ~32% of the Amazon rainforest's cover fraction[27]. *In situ* measurements were used to parameterise the models and to evaluate simulated ambient conditions (Extended Data Table 1, 2). Our aim was to generate *a priori* model-based hypotheses to highlight the state-of-the-knowledge and guide measurement strategies for

AmazonFACE and other ecosystem manipulation experiments to gain crucial process understanding of P control on the CO_2 fertilization effect.

Simulated eCO_2 (+200 ppm) had a positive effect on plant biomass C across all models but was weakest in the CNP models (Fig. 1a). The eCO_2 conditions induced average biomass C gains of 163 ± 65, 145 ± 83, and 79 ± 63 g C m^{-2} yr^{-1} (mean ± SD) over 15 years in the C, CN and CNP models, respectively (Fig. 1a). Limitations by P thus reduced the predicted biomass C sink by 52% and 46% compared to that in the C and CN models, respectively, with considerable variation across and within model groups (Extended Data Fig. 1). Plot inventories at the AmazonFACE site during the 2000s indicate an aboveground biomass increment of 23 g C m^2 yr^{-1}, substantially below the Amazon-wide[1] estimate of 64 g C m^2 yr^{-1}. The model ensemble represents ambient conditions, such as productivity and leaf area index, reasonably well, but ensemble members show divergence in other ecosystem characteristics, such as the biomass C increment, which range from 5 to 114 g C m^2 yr^{-1}. There is, however, no clear pattern in performance between the model groups, so that we judge that these differences do not have bearing on the conclusions of our study (see more discussion in Extended Data Fig. 2).

Differing model responses to phosphorus limitation

Gross and net primary productivity (GPP and NPP, respectively) are both stimulated by eCO_2 in all models, both initially (after 1 year of eCO_2) and until the end of the simulation. The CNP models show the strongest decline from the initial response due to P limitation (Fig. 1b, c). The final response of NPP to eCO_2 was a 35%, 29%, and 9% stimulation for the C, CN and CNP models, respectively. In general, in the CN and CNP models, nutrient limitation is defined as nutrient demand being greater than nutrient supply. However, models differ in their assumptions on how nutrient limitation controls productivity and C allocation in response to eCO_2, so that divergent responses on plant carbon use efficiency (CUE = NPP / GPP) are

simulated (Extended Data Table 3). In some CN models, CUE increases because N limitation is hypothesized to reduce autotrophic respiration (Ra) via lower tissue N content. Some CNP models, however, assume a direct downregulation of growth and hence the plant CUE decreases (Extended Data Fig. 3). Elevated CO_2 induced higher fine root investments of NPP in some CN and CNP models to aid nutrient acquisition (Fig. 1c; Extended Data Fig. 4). Predicted changes in allocation with eCO_2 cause a general increase in biomass turnover across all but one of the models, partially offsetting the positive biomass response (Extended Data Table 4). Changes in turnover play a minor role in our 15 years simulation period but rather control the long-term future CO_2 effect on the biomass C sink[28,29].

Plant growth under eCO_2 is lowest in CNP models as the low availability of soil labile P restricts P uptake either immediately or over time (Extended Data Fig. 5). We considered the modelled P limitation on plant growth to be realistic, as the models and observations agree on soil labile P being very low (Extended Data Fig. 2). Other site observations support the fact that P is extremely critical for plant productivity, such as high leaf N:P ratios of 37 and high plant P resorption (before litter fall) of 78% (Extended Data Table 1). While P limitation consistently reduces the eCO_2-induced biomass C sink, there is significant variation among CNP models due to contrasting process representations (Fig. 2; Extended Data Table 3). P shortages downregulate growth (i.e., NPP) in all CNP models, directly or via photosynthesis. The major differences in the model assumptions relate to how they modify P supply and demand to alleviate plant P shortages, including either (i) enhancing plant P use efficiency (PUE = NPP / P uptake) or (ii) upregulating P acquisition mechanisms. The models assume that PUE may change if tissue nutrient ratios are flexible, if C allocation changes among tissues with different stoichiometry, and/or if P resorption is variable (Fig. 2). Flexible stoichiometry is considered in all CNP models except ELM-CTC, although with varying

151 degrees of flexibility. Greater fine root C allocation with plant P stress is considered in some,
152 and P resorption is a fixed fraction of leaf tissue P in all models (Fig. 2).

153 Models differ in their representation of soil P acquisition mechanisms; three of the six models
154 (ELM-ECA, ELM-CTC, GDAY) consider desorption of P from mineral surfaces (i.e., the
155 secondary or strongly sorbed P pool), whereas the others assume P in those pools to be
156 unavailable to plants. All the models include biochemical mineralization of organic P via
157 phosphatase, but only three (ELM-ECA, ELM-CTC and ORCHIDEE) include the
158 functionality to increase P acquisition via this mechanism under plant P stress (Fig. 2;
159 Extended Data Table 3). Litter and soil stoichiometry are considered with varying degrees of
160 flexibility. Soil labile P limits microbial decomposition rates of litter and soil, so that
161 decomposition is reduced when immobilization demands for P exceed soil labile P availability
162 (Fig. 2; Extended Data Table 3).

163 **Enhanced phosphorus use efficiency and acquisition due to eCO_2**

164 Diverging representations of plant P use and acquisition among the CNP models cause
165 predictions of the eCO_2-induced biomass C sink to range from 5 g C m^{-2} yr^{-1} to 140 g C m^{-2}
166 yr^{-1} (Fig. 3a; Extended Data Fig. 1). Greater plant PUE occurred in four of the models, for
167 which shifts in tissue C:N and N:P due to eCO_2 led to increases in biomass C:P ranging from
168 ~200 to 1600 g C g P^{-1} (Fig. 3c). Higher fine root investment with eCO_2, at the expense of less
169 "P-costly" wood, offset some increases in PUE in some models. Flexible biomass
170 stoichiometry altered decomposition dynamics and induced progressive P limitation in
171 response to eCO_2, i.e., litter stoichiometry shifted towards lower quality (less N and P in
172 relation to C), reducing net P mineralization rates from microbial decomposition, causing P to
173 become increasingly unavailable to plants and accumulating in soil organic matter (Fig. 3d, e).
174 This plant-soil-microbial feedback slowed the cycling of P in the ecosystem and exacerbated
175 the initial P limitation (see Ref. [30] for a similar feedback during pedogenesis).

Enhanced plant P acquisition under eCO_2 effectively alleviated P limitation in two CNP models (ELM-CTC and ELM-ECA) (Fig. 3e). In both, eCO_2 increased the liberation of P from the secondary pool, as higher plant P demand and uptake diminished the labile P pool, in turn causing higher desorption rates. P desorption is thus only indirectly, and not mechanistically, enhanced by plants in these models. Biochemical mineralization of P under eCO_2 responded positively in both of the models, but added only notably to additional P acquisition in ELM-CTC (Fig. 3e). Although three CNP models simulated higher fine root investments, the actual P uptake return per fine root increment was marginal or came only into effect in the long-term (Extended Data Fig. 6).

Observations document ample N cycling in the system, e.g., high leaf N contents, indicative $\delta^{15}N$ values, high rates of N oxide emissions, and low leaf N resorption[31,32], and thereby suggest that plant growth is not directly affected by N availability. The CN models, however, simulate increased nitrogen use efficiency (NUE) and biomass C:N ratios, in response to insufficient N uptake under eCO_2 (Extended Data Fig. 5). Plant N availability may be underestimated in the models, since the plant-available mineral N supply was <7 g N m^{-2} across all models, as opposed to 17.5 g N m^{-2} observed in the top 10 cm only (Extended Data Fig. 2). These results highlight an important gap in our knowledge also related to the dynamics of N availability, and its potential interaction with P dynamics (Table 1).

Model-based hypotheses for the AmazonFACE experiment

In summary, the model ensemble encapsulates a range of plausible hypotheses and represents a potential range of biomass C responses to eCO_2 under low soil P availability. The assumption of a lacking ability of plants to acquire more soil P and a limited capacity for plants to use P more efficiently resulted in effectively zero biomass C gain with eCO_2. Conversely, flexible stoichiometry, in combination with enhanced plant P acquisition, were the key mechanistic responses leading to biomass gain with eCO_2. Divergences in the

simulated eCO_2 response lead us to the following testable hypotheses, and call for directed field measurements (Table 1):

H1. Low soil P availability will strongly constrain future plant biomass growth response to eCO_2 either by downregulating photosynthesis or limiting plant growth directly, or a combination thereof.

H2. Despite the limited soil P supply, plasticity in vegetation stoichiometry and allocation patterns will allow for some biomass growth under eCO_2.

H3. Plants will increase investments in P acquisition to increase P supply and allow biomass growth under eCO_2 either via greater P interception through fine root production or via greater P liberation from P desorption or biochemical mineralization of P.

These model-based hypotheses deepen a previous analysis of potential N and P limitation on C accumulation based on mass balance principle[33]. Furthermore, we add to a model intercomparison carried out in advance of the EucFACE experiment[34] by extending the range of plant P feedbacks considered across CNP models. This work highlighted H1: two stoichiometrically constrained CNP models predicted that strong P limitation will curtail the growth response to eCO_2 in Australia. Consistent with this hypothesis, aboveground growth has not increased with eCO_2 in that experiment over the initial years[35]. This finding underlines that monitoring efforts need to place a strong(er) focus on belowground carbon and nutrient dynamics, in addition to canopy-scale photosynthesis and aboveground growth dynamics. Additionally, Ra dependence on P content and plant stress from drought or nutrient limitation need further monitoring during experiments to fully elucidate the plant C budget and address H1 (Table 1).

Nutrient fertilization experiments support H2, as plasticity in leaf stoichiometry at the individual level, along with plasticity in P resorption efficiency, was observed[36]. Across the

225 Amazon, community-weighted leaf N:P in the field varied from 13 to 42 g N g P^{-1} (n = 64)
226 (Ref. [32]), which place our site, with a mean of 37, closer to the high end. GDAY predicted the
227 most plausible increase in the leaf N:P ratio from 34 to 38 (Extended Data Fig. 7). Two
228 models predicted strong increases in the leaf N:P ratio with eCO_2 but started off with much
229 lower initial values. The degree to which plasticity in stoichiometry and resorption can aid
230 plant PUE under eCO_2 in highly P-limited sites that are already at the end of the observed
231 spectrum remains to be seen (H2). Monitoring plant tissue stoichiometry, including wood
232 with much higher N:P ratios, combined with assessments of P resorption in CO_2 and nutrient
233 fertilization experiments will reduce uncertainties (Table 1).

234 Based on previous observations[8], a number of models assume increased fine root investment,
235 as well as higher biochemical P mineralization and P desorption from mineral surfaces, under
236 eCO_2-induced nutrient limitation (H3). The effect of increased fine root biomass on nutrient
237 uptake was limited in our simulations and ambient fine root allocation fractions were highly
238 variable among the models, ranging from 5-30% of NPP (Extended Data Fig. 4, 6). Both these
239 modelled results highlight model deficiencies in belowground processes[37] that need
240 addressing (Table 1). There is evidence that phosphatase activity in litter and soil and the
241 presence of low-molecular-weight acids used to liberate P from organic matter or from
242 mineral surfaces increase with plant P demand[38]. This was predicted by ELM-CTC in our
243 simulations, which also showed Amazon-wide that "[with] enhanced phosphatase production,
244 productivity in the highly P-limited areas can be sustained under elevated CO_2 conditions"[39].
245 Plants invest in P liberation and acquisition, but if these mechanisms can be upregulated under
246 eCO_2 and over what time frame this may occur remain open questions. Quantification of such
247 a response is lacking, as are estimates of the associated plant C costs to acquire P via these
248 and other mechanisms, such as mycorrhizal symbiosis[15,40] (Table 1). The P gain and C cost
249 for P acquisition mechanisms, as well as the associated plant-soil-microbial interactions, need

to be assessed by analyses of soil, microbial and root nutrition, and via novel techniques investigating enzyme and labile C dynamics[41]. Monitoring of belowground fine root dynamics needs to include the surface litter layer, commonly explored by fine roots in P-impoverished ecosystems in the Amazon, not yet quantified nor considered in models (Table 1).

Implications of considering phosphorus for the CO_2 fertilization effect

Previous model projections suggest a sustained fertilization effect of CO_2 on the Amazon C sink but have not considered feedbacks from low soil P availability[5,6]. Our study demonstrates that, based on the current generation of CNP models, the omission of P feedbacks is highly likely to cause an overestimation of the Amazon rainforest's capacity to sequester atmospheric CO_2. Considering P limitation on the CO_2 fertilization effect in future predictions may indicate that the forest is less resilient to higher temperatures and changing rainfall patterns than previously thought[6,42]. Periods of water deficit may contribute to the eCO_2 fertilization effect on productivity due to its water saving effect[34], or due to alterations of decomposition processes. Our study site experienced years with significantly less than average precipitation, e.g. in 2000 and 2009, however, in our simulations this increased the positive response of GPP and NPP to eCO_2 only marginally (Extended Data Figure 8 and 9). Models lack the appropriate sensitivity of plant responses to changes in water availability, and even more so when precipitation sums are that high[43]. Interactions of water and P availability and their consequences on the CO_2 fertilization effect remain uncertain[44] and is an area where field measurements will allow us to better constrain model responses (Table 1).

Although P is likely to reduce the biomass C sink response to CO_2 in regions with low plant-available P supply, our results suggest that plasticity in plant P use and plant P acquisition mechanisms, may at least partially alleviate P limitation under eCO_2 and enable CO_2 fertilization of biomass growth. The model ensemble may be interpreted as representing a

range of possible tropical plant functional strategies and growth responses to low P availability under eCO_2. Responses are expected to be species-specific, as were plant growth responses to low P supplies in another tropical region[18]. The ecosystem-scale response to P limitation under eCO_2 will thus depend on the relative contributions of the various P acquisition and P use strategies across individuals, their interactions and to what extent these processes can be upregulated under eCO_2. All of which ultimately need to be described and represented in a single model framework in order to accurately predict the Amazon rainforest's response to future climate change.

AmazonFACE has the unique opportunity to experimentally address these key areas of uncertainty, not only by integrating the proposed measurements across seasons and at the ecosystem scale (summary in Table 1) but also by assessing species-specific responses to eCO_2 in relation to trait expression. Amazon-wide expression of plant functional strategies may then be inferred by applying the mechanistic interplay between trait expression and edaphic conditions. The key to predicting the future of the world's largest tropical forest under eCO_2 thus lies in obtaining experimental data on, and subsequently modelling, different plant P acquisition and use strategies, as well as their interactions in a competing plant community.

REFERENCES

1. Brienen, R. J. W. *et al.* Long-term decline of the Amazon carbon sink. *Nature* **519,** 344–348 (2015).

2. Phillips, O. L. & Brienen, R. J. W. Carbon uptake by mature Amazon forests has mitigated Amazon nations' carbon emissions. *Carbon Balance Manag.* **12,** 1 (2017).

3. Cernusak, L. A. *et al.* Tropical forest responses to increasing atmospheric CO2: Current knowledge and opportunities for future research. *Funct. Plant Biol.* **40,** 531–551 (2013).

4. Ciais, P. *et al.* The physical science basis. Contribution of working group I to the fifth assessment report of the intergovernmental panel on climate change. *Chang. IPCC Clim.* 465–570 (2013).

5. Cox, P. M. *et al.* Sensitivity of tropical carbon to climate change constrained by carbon dioxide variability. *Nature* **494,** 341–344 (2013).

6. Huntingford, C. *et al.* Simulated resilience of tropical rainforests to CO$_2$-induced climate change. *Nat. Geosci.* **6,** 268–273 (2013).

7. Talhelm, A. F. *et al.* Elevated carbon dioxide and ozone alter productivity and ecosystem carbon content in northern temperate forests. *Glob. Chang. Biol.* **20,** 2492–2504 (2014).

8. Norby, R. J., Warren, J. M., Iversen, C. M., Medlyn, B. E. & McMurtrie, R. E. CO2 enhancement of forest productivity constrained by limited nitrogen availability. *Proc. Natl. Acad. Sci.* **107,** 19368–19373 (2010).

9. Zaehle, S. *et al.* Evaluation of 11 terrestrial carbon-nitrogen cycle models against observations from two temperate Free-Air CO2Enrichment studies. *New Phytol.* **202,**

803–822 (2014).

10. Hofhansl, F. *et al.* Amazon forest ecosystem responses to elevated atmospheric CO2 and alterations in nutrient availability: filling the gaps with model-experiment integration. *Front. Earth Sci.* **4,** (2016).

11. Norby, R. J. *et al.* Model-data synthesis for the next generation of forest free-air CO2 enrichment (FACE) experiments. *New Phytol.* **209,** 17–28 (2016).

12. Lloyd, J., Bird, M. I., Veenendaal, E. M. & Kruijt, B. Should Phosphorus Availability Be Constraining Moist Tropical Forest Responses to Increasing CO2 Concentrations? *Glob. Biogeochem. Cycles Clim. Syst.* 95–114 (2001).

13. Vitousek, P. M. Litterfall, nutrient cycling, and nutrient limitation in tropical forests. *Ecology* **65,** 285–298 (1984).

14. Quesada, C. A. *et al.* Basin-wide variations in Amazon forest structure and function are mediated by both soils and climate. *Biogeosciences* **9,** 2203–2246 (2012).

15. Lambers, H., Raven, J. A., Shaver, G. R. & Smith, S. E. Plant nutrient-acquisition strategies change with soil age. *Trends Ecol. Evol.* **23,** 95–103 (2008).

16. Reed, S. C., Yang, X. & Thornton, P. E. Incorporating phosphorus cycling into global modeling efforts: A worthwhile, tractable endeavor. *New Phytol.* **208,** 324–329 (2015).

17. Jiang, M., Caldararu, S., Zaehle, S., Ellsworth, D. S. & Medlyn, B. E. Towards a more physiological representation of vegetation phosphorus processes in land surface models. *New Phytol.* 1–7 (2019).

18. Turner, B. L., Brenes-Arguedas, T. & Condit, R. Pervasive phosphorus limitation of tree species but not communities in tropical forests. *Nature* **555,** 367–370 (2018).

19. Goll, D. S. *et al.* A representation of the phosphorus cycle for ORCHIDEE (revision

4520). *Geosci. Model Dev.* **10,** 3745–3770 (2017).

20. Wang, Y.-P., Law, R. M. & Pak, B. A global model of carbon, nitrogen and phosphorus cycles for the terrestrial biosphere. *Biogeosciences* **7,** 2261–2282 (2010).

21. Haverd, V. *et al.* A new version of the CABLE land surface model (Subversion revision r4601) incorporating land use and land cover change, woody vegetation demography, and a novel optimisation-based approach to plant coordination of photosynthesis. *Geosci. Model Dev.* **11,** 2995–3026 (2018).

22. Comins, H. N. & McMurtrie, R. E. Long-Term Response of Nutrient-Limited Forests to CO2 Enrichment; Equilibrium Behavior of Plant-Soil Models. *Ecol. Appl.* **3,** 666–681 (1993).

23. Zhu, Q., Riley, W. J., Tang, J. & Koven, C. D. Multiple soil nutrient competition between plants, microbes, and mineral surfaces: model development, parameterization, and example applications in several tropical forests. *Biogeosciences* **13,** 341–363 (2016).

24. Yang, X., Thornton, P. E., Ricciuto, D. M. & Post, W. M. The role of phosphorus dynamics in tropical forests – a modeling study using CLM-CNP. *Biogeosciences* **11,** 1667–1681 (2014).

25. Malhi, Y. *et al.* Comprehensive assessment of carbon productivity, allocation and storage in three Amazonian forests. *Glob. Chang. Biol.* **15,** 1255–1274 (2009).

26. Araújo, A. C. *et al.* Comparative measurements of carbon dioxide fluxes from two nearby towers in a central Amazonian rainforest: The Manaus LBA site. *J. Geophys. Res.* **107,** 8090 (2002).

27. Quesada, C. A. *et al.* Soils of Amazonia with particular reference to the RAINFOR sites. *Biogeosciences* **8,** 1415–1440 (2011).

28. Friend, A. D. *et al.* Carbon residence time dominates uncertainty in terrestrial vegetation responses to future climate and atmospheric CO_2. *Proc. Natl. Acad. Sci.* **111,** 3280–3285 (2014).

29. Walker, A. P. *et al.* Predicting long-term carbon sequestration in response to CO2 enrichment: How and why do current ecosystem models differ? *Global Biogeochem. Cycles* **29,** 476–495 (2015).

30. Vitousek, P. M. *Nutrient cycling and limitation: Hawai'i as a model system*. *Princeton University Press* (2004).

31. Nardoto, G. B. *et al.* Basin-wide variations in Amazon forest nitrogen-cycling characteristics as inferred from plant and soil 15N:14N measurements. *Plant Ecol. Divers.* **7,** 173–187 (2014).

32. Fyllas, N. M. *et al.* Basin-wide variations in foliar properties of Amazonian forest: phylogeny, soils and climate. *Biogeosciences* **6,** 2677–2708 (2009).

33. Wieder, W. R., Cleveland, C. C., Smith, W. K. & Todd-Brown, K. Future productivity and carbon storage limited by terrestrial nutrient availability. *Nat. Geosci.* **8,** 441–444 (2015).

34. Medlyn, B. E. *et al.* Using models to guide field experiments: a priori predictions for the CO2 response of a nutrient- and water-limited native Eucalypt woodland. *Glob. Chang. Biol.* **22,** 2834–2851 (2016).

35. Ellsworth, D. S. *et al.* Elevated CO2 does not increase eucalypt forest productivity on a low-phosphorus soil. *Nat. Clim. Chang.* **7,** 279–282 (2017).

36. Wright, S. J. *et al.* Plant responses to fertilization experiments in lowland, species-rich, tropical forests. *Ecology* **99,** 1129–1138 (2018).

37. Warren, J. M. *et al.* Root structural and functional dynamics in terrestrial biosphere models--evaluation and recommendations. *New Phytol.* **205,** 59–78 (2015).

38. Hoosbeek, M. R. Elevated CO2 increased phosphorous loss from decomposing litter and soil organic matter at two FACE experiments with trees. *Biogeochemistry* **127,** 89–97 (2016).

39. Yang, X., Thornton, P. E., Ricciuto, D. M. & Hoffman, F. M. Phosphorus feedbacks constraining tropical ecosystem responses to changes in atmospheric CO2 and climate. *Geophys. Res. Lett. Res.* 7205–7214 (2016).

40. Vicca, S. *et al.* Fertile forests produce biomass more efficiently. *Ecol. Lett.* **15,** 520–526 (2012).

41. Wang, Y. & Lambers, H. Root-released organic anions in response to low phosphorus availability: recent progress, challenges and future perspectives. *Plant Soil* (2019). doi:10.1007/s11104-019-03972-8

42. Gatti, L. V. *et al.* Drought sensitivity of Amazonian carbon balance revealed by atmospheric measurements. *Nature* **506,** (2014).

43. Powell, T. L. *et al.* Confronting model predictions of carbon fluxes with measurements of Amazon forests subjected to experimental drought. *New Phytol.* **200,** 350–365 (2013).

44. He, M. & Dijkstra, F. A. Drought effect on plant nitrogen and phosphorus: A meta-analysis. *New Phytol.* **204,** 924–931 (2014).

ACKNOWLEDGEMENTS

The AmazonFACE research program provided logistical support to conduct this study (https://amazonface.inpa.gov.br/). This study was funded by the Inter-American Development Bank through a technical cooperation agreement with the Brazilian Ministry of Science, Technology, Innovation and Communications (Grant BR-T1284), by Brazil's Coordination for the Improvement of Higher Education Personnel (CAPES) Grant 23038.007722/2014-77, by Amazonas Research Foundation (FAPEAM) Grant 2649/2014 and São Paulo Research Foundation (FAPESP) Grant 2015/02537-7. We thank the many scientists, field and laboratory technicians, students and other personnel involved in the development of the models, in collecting and analysing the field data, or in the planning and execution of the AmazonFACE program. We thank the German Research Foundation (DFG) for financing one of the workshops that made this study possible (grant No. RA 2060/4-1). TFD, SG, AG and CAQ thank the USAID for funding via the PEER program (grant agreement AID-OAA-A-11-00012). APW and RJN were supported the FACE Model-Data Synthesis project, XY and QZ were supported by the Energy Exascale Earth System (E3SM) program and JAH was supported by the Next Generation Ecosystem Experiments-Tropics project; all funded by the U.S. Department of Energy, Office of Science, Office of Biological and Environmental Research under contract numbers DE-AC02-05CH11231 and DE-AC05-00OR22725. MDK acknowledges support from the Australian Research Council Centre of Excellence for Climate Extremes (CE170100023) and the New South Wales Research Attraction and Acceleration Program. YPW, BP and VH acknowledge the support from the National Earth System Science Program of the Australian Government. DSG is funded by the "IMBALANCE-P" project of the European Research Council (ERC-2013-SyG-610028). LMM acknowledges funding from the UK's Natural Environment Research Council (NERC) grant numbers

NE/LE007223/1 and NE/N017951/1. FL acknowledges funding from EU FP7 LUC4C program (GA603542). KF is funded by the DFG (grant No. RA 2060/5-1.).

AUTHOR CONTRIBUTIONS

DML, AR, and KF conceived the study. LF, SG, AG, FH, RN, CAQ, KJS, and OJV-B collected field data. KF, DG, MDK, MJ, VH, JAH, FL, LMM, BP, CvR, Y-PW, XY, SZ, and QZ performed model simulations. KF wrote the manuscript with contributions from all co-authors.

COMPETING INTERESTS

The authors declare no financial or non-financial competing interests.

ADDITIONAL INFORMATION

Site data used for model evaluation and calibration are available in the Supplementary Information. Model driving data can be obtained upon request by CvR. Correspondence and request for material should be addressed to KF (katrin.fleischer@tum.de).

FIGURE CAPTIONS

Figure 1. The predicted effect of eCO_2 on biomass C, productivity and biomass compartments for C, CN and CNP models. (a), The final response of biomass growth, calculated as the mean annual response over 15 years of eCO_2 in g C m^{-2} yr^{-1}. (b), first-year response of productivity (GPP and NPP), and CUE (=NPP/GPP) in %. c), 15-year response of productivity, CUE, and leaf, fine root and wood C (calculated as mean response of 13^{th} to 17^{th} year), all in %. Responses to eCO_2 are the differences between the elevated and ambient model run, shown as mean and standard deviation per model group, and individual model results as dots.

Figure 2. Strength of phosphorus feedbacks in controlling the biomass C response to eCO_2 for the six CNP models. The degree to which modelled P feedback on ecosystem processes control the response of biomass C to eCO_2 in our simulations (none, intermediate, high). P limitation downregulates photosynthesis or growth under eCO_2 in all models. Maintenance respiration, leaf turnover and P resorption are not responsive to P feedbacks in any of the models. Leaf N:P responds to eCO_2 in most models. Desorption of P from mineral surfaces is only considered in ELM-ECA and ELM-CTC, and biochemical P mineralization is considered in many models, but effectively responsive only in ELM-CTC. See also Extended Data Table 3.

Figure 3. Key responses of biomass C gain, stoichiometry, allocation, and P dynamics to eCO_2 for the CNP models (blue=positive, red=negative). (a), Mean annual change in standing leaf, fine root and wood C over 15 years, increasing across models from left to right in g C m^{-2} yr^{-1}. (b), The mean change in C allocation for fine roots and wood in %. (c), Mean change in tissue stoichiometry in absolute terms in g C g P^{-1} and change in P use efficiency over 15 years in g C g P^{-1} yr^{-1}. (d), Mean change in ecosystem P input and output (leaching) fluxes in g P m^{-2} yr^{-1} and in final P stock in biomass, organic soil, mineral soil and total

ecosystem in g P m^{-2}. (e), Mean change in plant P acquisition processes, including net P mineralization, biochemical P mineralization and P uptake in g P m^{-2} yr^{-1}, and secondary and labile P pools in g P m^{-2}. For both, (d) and (e), P flux changes are differences of cumulative fluxes after 15 years and P pool changes are differences in pools after 15 years.

METHODS

Site description

Model simulations were conducted at the AmazonFACE experimental site in Central Amazonia (2º35'39" S, 60º12'29'' W). AmazonFACE is an integrated model-experiment project that aims to assess the effects of high CO_2 concentrations on the ecology and resilience of the Amazon rainforest (http://amazon-face.org/). The experiment is currently being established and is situated in a *terra firme* forest on a plateau characterized by highly weathered, deep, clay sediment soil (with a clay fraction of 76%), classified as a Geric Ferrasol[45]. The site and the surrounding area have been subjected to various long-term measurement activities[25,46–49], coordinated by the Large-Scale Biosphere-Atmosphere Program (LBA; http://lba2.inpa.gov.br/) in Amazonia, including the "K34" eddy covariance flux tower[26], located approximately 2 km away from AmazonFACE site. Mean annual precipitation at K34 from January 2000 to December 2015 was 2600 mm yr^{-1}, and the mean temperature was 26°C.

Model descriptions

Fourteen ecosystem models with contrasting representations of ecosystem functioning and nutrient cycling were applied to the experiment (Extended Data Table 3). C cycle dynamics without nutrient cycle feedbacks are represented in the "C-only" models (InLand, ED2 and ELM-FATES)[50–52]; C and N dynamics are represented in the "CN" models (LPJ-GUESS, O-CN, JULES, CABLE-POP(CN) and GDAY(CN))[53–55]; and C, N, and P dynamics are represented in the "CNP" models (ELM-ECA, ELM-CTC, CABLE, CABLE-POP, ORCHIDEE, and GDAY)[19–24]. Two models were included with a respective CN and CNP version (GDAY and CABLE-POP) to directly assess the effect of considering P dynamics. The other models were treated as a non-random sample from the possible C, CN, and CNP modelling assumptions. Four of the models are dynamic vegetation models: CABLE-POP

considers dynamic establishment and mortality with fixed plant functional type (PFT) composition, while LPJ-GUESS, ED2 and ELM-FATES also consider dynamic PFT composition. Photosynthesis is based on formulations by Farquahar[56] or derivations thereof in all of the models[57,58] (Extended Data Table 3).

Prognostic C allocation fractions are based on functional relationships among tissues, e.g., fixed ratios between sapwood and leaf area in CABLE-POP, LPJ-GUESS, ED2, GDAY, ORCHIDEE, O-CN, JULES, and ELM-FATES, and on resource dependence, e.g., higher root allocation under water or nutrient stress in LPJ-GUESS, ELM-ECA, GDAY, O-CN, ORCHIDEE, ED2 and ELM-FATES. C allocation fractions are fixed in InLand and CABLE.

Nutrient limitation is determined by the difference between demand and supply (via root uptake and resorption) of N or P, with the most limiting nutrient determining the degree of limitation. The photosynthetic parameters V_{cmax} and/or J_{max} are controlled by leaf N in all CN and CNP models except JULES, while leaf P additionally downregulates gross primary productivity (GPP) in all CNP models except ORCHIDEE. N controls net primary productivity (NPP) in some of the models, i.e., O-CN, JULES, ORCHIDEE, CABLE and CABLE-POP, and additionally downregulates growth efficiency (GPP/LAI) in CABLE and CABLE-POP.

Maintenance respiration is dependent on temperature in all models and is additionally controlled by tissue N content in all of the models that consider the N cycle with the exception of GDAY, where Ra is a fixed fraction of GPP. Plant tissue stoichiometry in the CN and CNP models is either fixed (ELM-CTC and JULES) or varies within or without bounds (all other models). The nutrient resorption rates in the CN and CNP models are always fixed fractions of the nutrient content in leaves and roots. Competition for nutrients between plant uptake and decomposition processes is handled differently. Nutritional demands for the decomposition process (representing microbial demands) are met entirely first in some models (CABLE, O-

CN, ORCHIDEE, and GDAY), are based on relative demands between decomposition and plant uptake (ELM-CTC), or are determined via a multiple consumer approach including adsorption to mineral surfaces (ELM-ECA). Nutrient uptake is a function of plant demand and nutrient availability in all models and is further controlled by a measure of root mass in LPJ-GUESS, GDAY, ORCHIDEE, and O-CN.

Soil organic matter (SOM) decomposition is limited by soil mineral N availability in most CN and CNP models (except O-CN and ORCHIDEE) and additionally by labile P availability in most CNP models (except GDAY and ORCHIDEE). P in SOM can also be mineralized via phosphatase, decoupling the P cycle from the C and N cycle, termed biochemical P mineralization in the P models. Biochemical P mineralization is a function of the slow SOM pool turnover in CABLE, CABLE-POP and GDAY, as well as substrate availability in ORCHIDEE, ELM-ECA and ELM-CTC. Biochemical P mineralization is upregulated with higher plant P stress, representing higher phosphate production (not specified if by plants or microbes), in ELM-ECA, ELM-CTC and ORCHIDEE.

N inputs originate from N deposition (prescribed by model protocol) and N fixation (prescribed individually). N fixation is either fixed, calculated empirically as a fraction of NPP or evapotranspiration (GDAY, JULES, ORCHIDEE, ELM-CTC, LPJ-GUESS, CABLE, and CABLE-POP), or based on an optimization scheme (ELM-ECA and O-CN). P inputs originate from weathering (prescribed individually) and deposition (prescribed by model protocol). Release of P from rock weathering is a fixed, soil type-specific rate in CABLE and CABLE-POP, a function of the parent P pool in ELM-ECA, ELM-CTC, and GDAY or described as a function of lithology, runoff and air temperature in ORCHIDEE. N and P losses occur from leaching, modelled as a function of the size of the labile P and mineral N pool, respectively, and additionally controlled by runoff in ELM-ECA and ORCHIDEE.

The number of inorganic P pools and their precise definition varies among the models. We consider two inorganic P pools relevant for our analysis: the labile P pool and the secondary P pool. The labile P pool encompasses plant-available inorganic P, represented in most CNP models by two separate pools connected by sorption dynamics and effectively in equilibrium (described by Langmuir dynamics in most models and a linear approach in ORCHIDEE). The labile P pools follow different nomenclature in the models but are comparable in functionality: the P in soil solution (called labile or solution P) is readily available to plants in the model time step, while the non-dissolved P (referred to as sorbed or sorbed labile P pool) can become available to plants on yearly to decadal time scales due to desorption. The secondary P pool represents P strongly sorbed by minerals, which is largely unavailable but may enter the labile P pool on centennial time scales and, depending on model assumptions, may be driven by plant P stress.

Model simulations

Models were forced with 16 years of observed local meteorology (2000 to 2015) from the K34 flux tower[26]. Meteorological data from July 1999 to December 2015 of near-surface air temperature, rainfall, downward shortwave radiation, downward longwave radiation, vapour pressure deficit, surface pressure, relative humidity, and wind speed were available for model input. Specific humidity was calculated based on observed relative humidity and surface pressure. All data time series were subject to quality control (i.e., removal of outliers) and gap filling using the variables' climatological mean. Precipitation data gaps were filled from a nearby weather station of the Tropical Rainfall Measuring Mission network.

Simulations are initialized with a spin-up routine resulting in equilibrium conditions of C stocks (and N, and P, if applicable) representing the year 1850. The 16-year meteorological time series are continuously repeated throughout the whole spin-up, during the transient phase (1851 to 1998), and during our model-experiment phase (1999 to 2013), representative of a

570 15-year long AmazonFACE experiment. Global datasets are used as inputs for atmospheric
571 CO_2[59,60], N deposition[61,62], and P deposition[63]. Atmospheric CO_2, N and P deposition levels
572 were set to 284.7 ppm, 1.43 kg N ha^{-1} yr^{-1}, and 0.144 kg P ha^{-1} yr^{-1} in 1850, respectively, and
573 follow historical changes during the transient and model experiment phase.

574 Other site parameters used for parameterization of the models are derived from *in situ*
575 measurements and include rooting and soil depth (set to rooting depth), soil hydraulic
576 parameters, specific leaf area (SLA), and soil texture (Extended Data Table 2). Soil hydraulic
577 parameters are derived from pedotransfer functions[64] and site-specific measurements of soil
578 properties[65]. Soil hydraulic parameters were included in models that accounted for this
579 functionality to allow for a better representation of soil water dynamics in tropical soils
580 (Extended Data Table 2).

581 Two model experiments are performed over the 15-year long experiment phase by each model
582 to assess the effect of elevated CO_2: 1) the ambient run (AMB) and 2) the elevated CO_2 run
583 (ELE). In the AMB run, the atmospheric CO_2 is set to ambient levels and is employed for
584 model evaluation against *in situ* measurements, including C fluxes from the K34 flux tower.
585 The ELE run represents the planned AmazonFACE experiment with a step change increase of
586 200 ppm at the start of the model experiment and continuous tracking of CO_2 levels in AMB
587 plus 200 ppm thereafter. Model outputs are analysed in biological years of seasonality (July to
588 June), and the difference between the elevated CO_2 run and the control run are used to infer
589 the model-based CO_2 effect.

590 **Model output analysis**

591 The analysis of the modelled output includes the evaluation of modelled ambient conditions
592 relative to *in situ* observations and hypotheses-based analyses of the modelled CO_2 responses.
593 We employ a structural analysis of the model simulations[9,66–68], splitting model outcomes into
594 the underlying processes to identify crucial model assumptions determining diverging

predictions for the FACE experiment. We focus on the simulated increase in biomass C due to eCO_2 and the underlying nutrient control thereon.

Biomass C dynamics are a result of primary productivity, C allocation and turnover. We first analyse the effect of eCO_2 on gross primary productivity (GPP), net primary productivity (NPP), autotrophic respiration (Ra), and the resulting plant carbon use efficiency (CUE), where CUE = NPP/GPP. We then assess changes in NPP allocation fractions to biomass compartments of wood, fine roots and leaves, and the resulting effect on biomass C turnover in response to eCO_2. Specific tissue turnover rates are fixed in all models, but overall biomass C turnover changes as a result of changing C allocation to tissue compartments. Turnover rates of biomass C pools are calculated as the fraction of total litter fall per total biomass pool size (Extended Data Table 4).

Plant nutrient cycle feedbacks to eCO_2 are assessed by splitting the responses into plant N uptake (NUP) and plant N use efficiency (NUE), where NUE = NPP/NUP, and similarly into P uptake (PUP) and P use efficiency (PUE), where PUE = NPP/PUP. The responses of NUE and PUE to eCO_2 are further split into changes in tissue C allocation (differing in C:N and N:P ratios) and changes in tissue stoichiometry (flexible C:N and N:P ratios). Soil nutrient cycle feedbacks to eCO_2 are determined by separating eCO_2 responses in N and P mineralization rates (N and P mineralization from microbial decomposition of SOM and biochemical P mineralization of organic P via phosphatase) and the balance of ecosystem N and P inputs (N fixation, N and P deposition, and P weathering) and losses (N and P leaching).

Data availability

Model output data used for analyses and figures have been archived in a GitHub repository (https://github.com/Kaaze7/AmzFACE-model-ensemble-2019).

Code availability

Code used for analyses and figures have been archived in a GitHub repository (https://github.com/Kaaze7/AmzFACE-model-ensemble-2019).

REFERENCES METHODS

45. Quesada, C. A. *et al.* Variations in chemical and physical properties of Amazon forest soils in relation to their genesis. *Biogeosciences* **7,** 1515–1541 (2010).

46. Chambers, J. Q. *et al.* Respiration from a Tropical Forest Ecosystem : Partitioning of Sources and Low Carbon Use Efficiency. *Ecol. Appl.* **14,** 72–88 (2004).

47. Aragão, L. E. O. C. *et al.* Above- and below-ground net primary productivity across ten Amazonian forests on contrasting soils. *Biogeosciences* **6,** 2759–2778 (2009).

48. Holm, J. A., Chambers, J. Q., Collins, W. D. & Higuchi, N. Forest response to increased disturbance in the central Amazon and comparison to western Amazonian forests. *Biogeosciences* **11,** 5773–5794 (2014).

49. Hadlich, H. L. *et al.* Recognizing Amazonian tree species in the field using bark tissues spectra. *For. Ecol. Manage.* **427,** 296–304 (2018).

50. Kucharik, C. J. *et al.* Testing the performance of a dynamic global ecosystem model: Water balance, carbon balance, and vegetation structure. *Global Biogeochem. Cycles* **14,** 795–825 (2000).

51. Fisher, R. A. *et al.* Taking off the training wheels: The properties of a dynamic vegetation model without climate envelopes, CLM4.5(ED). *Geosci. Model Dev.* **8,** 3593–3619 (2015).

52. Medvigy, D., Wofsy, S. C., Munger, J. W., Hollinger, D. Y. & Moorcroft, P. R. Mechanistic scaling of ecosystem function and dynamics in space and time: Ecosystem Demography model version 2. *J. Geophys. Res. Biogeosciences* **114,** (2009).

53. Smith, B. *et al.* Implications of incorporating N cycling and N limitations on primary production in an individual-based dynamic vegetation model. *Biogeosciences* **11,** 2027–2054 (2014).

54. Zaehle, S. & Friend, A. D. Carbon and nitrogen cycle dynamics in the O-CN land

surface model: 1. Model description, site-scale evaluation, and sensitivity to parameter estimates. *Global Biogeochem. Cycles* **24,** n/a-n/a (2010).

55. Best, M. J. *et al.* The Joint UK Land Environment Simulator (JULES), model description – Part 1: Energy and water fluxes. *Geosci. Model Dev.* **4,** 677–699 (2011).

56. Farquhar, G. D., von Caemmerer, S. & Berry, J. A. A biochemical model of photosynthetic CO2 assimilation in leaves of C3 species. *Planta* **149,** 78–90 (1980).

57. Collatz, G. J., Ball, J. T., Grivet, C. & Berry, J. A. Physiological and Environmental-Regulation of Stomatal Conductance, Photosynthesis and Transpiration - a Model That Includes a Laminar Boundary-Layer. *Agric. For. Meteorol.* **54,** 107–136 (1991).

58. Kull, O. & Kruijt, B. Leaf photosynthetic light response: A mechanistic model for scaling photosynthesis to leaves and canopies. *Funct. Ecol.* **12,** 767–777 (1998).

59. Etheridge, D. M. *et al.* Natural and anthropogenic changes in atmospheric CO2over the last 1000 years from air in Antarctic ice and firn. *J. Geophys. Res. Atmos.* **101,** 4115–4128 (1996).

60. MacFarling Meure, C. *et al.* Law Dome CO_2, CH_4 and N_2O ice core records extended to 2000 years BP. *Geophys. Res. Lett.* **33,** L14810 (2006).

61. Lamarque, J. F. *et al.* Historical (1850-2000) gridded anthropogenic and biomass burning emissions of reactive gases and aerosols: Methodology and application. *Atmos. Chem. Phys.* **10,** 7017–7039 (2010).

62. Lamarque, J. F. *et al.* Global and regional evolution of short-lived radiatively-active gases and aerosols in the Representative Concentration Pathways. *Clim. Change* **109,** 191–212 (2011).

63. Wang, R. *et al.* Global forest carbon uptake due to nitrogen and phosphorus deposition from 1850 to 2100. *Glob. Chang. Biol.* **23,** 4854–4872 (2017).

64. Tomasella, J. & Hodnett, M. Pedotransfer functions for tropical soils. in *Developments*

in Soil Science **30,** 415–429 (Elsevier, 2004).

65. Marthews, T. R. *et al.* High-resolution hydraulic parameter maps for surface soils in tropical South America. *Geosci. Model Dev.* **7,** 711–723 (2014).

66. De Kauwe, M. G. *et al.* Where does the carbon go? A model-data intercomparison of vegetation carbon allocation and turnover processes at two temperate forest free-air CO2enrichment sites. *New Phytol.* **203,** 883–899 (2014).

67. Walker, A. P. *et al.* Comprehensive ecosystem model□data synthesis using multiple data sets at two temperate forest free□air CO2 enrichment experiments: Model performance at ambient CO2 concentration. *J. Geophys. Res. Biogeosciences* **119,** 937–964 (2014).

68. Medlyn, B. E. *et al.* Using ecosystem experiments to improve vegetation models. *Nat. Clim. Chang.* **5,** 528–534 (2015).

684 Table 1. List of key processes and variables that need to be constrained by observational

685 estimates in order reduce uncertainty in P cycle control on the eCO_2 effect ecosystem models.

(H1) Plant C budget	**Measurements needed**
Canopy scale C assimilation	• Seasonal dynamics of leaf area and photosynthetic capacity • Photosynthetic acclimation
Plant tissue respiration	• Control of drought stress, nutrient limitation and P content • Wood and root respiration
Biomass growth	• Belowground biomass compartments • Long term growth rates
(H2) Plant P use	
Plant tissue C:P and N:P stoichiometry	• Plasticity versus adaptability to (experimental) change in eCO_2 or nutrient availability • Functionality of tissue P • Wood P content /stoichiometry
Plant tissue P resorption	• P content in live tissue and fresh litter • Plasticity versus adaptability to (experimental) change in eCO_2 or nutrient availability
(H3) Plant P acquisition	
P desorption due to plant exudation	• Interactions with microorganisms (directly or via microorganisms) • Cost of exudation vs. plant P uptake
P acquisition due to fine root production	• Surface litter activity • Fine root allocation fractions • Fine root productivity vs. plant P uptake
Biochemical P mineralization (via phosphatase)	• Phosphatase activity and relation to P mineralization • Plant production of phosphatase vs. plant-induced production by microorganisms • Cost of phosphatase production vs. plant P acquisition
Other interactions	
Plant N availability	• Ecosystem N budget • Symbiotic and free-living N fixation • Control of N availability on P acquisition
Plant water availability	• Control on P mineralization and transport dynamics • Control on of water and P limitation on eCO_2 effect

686

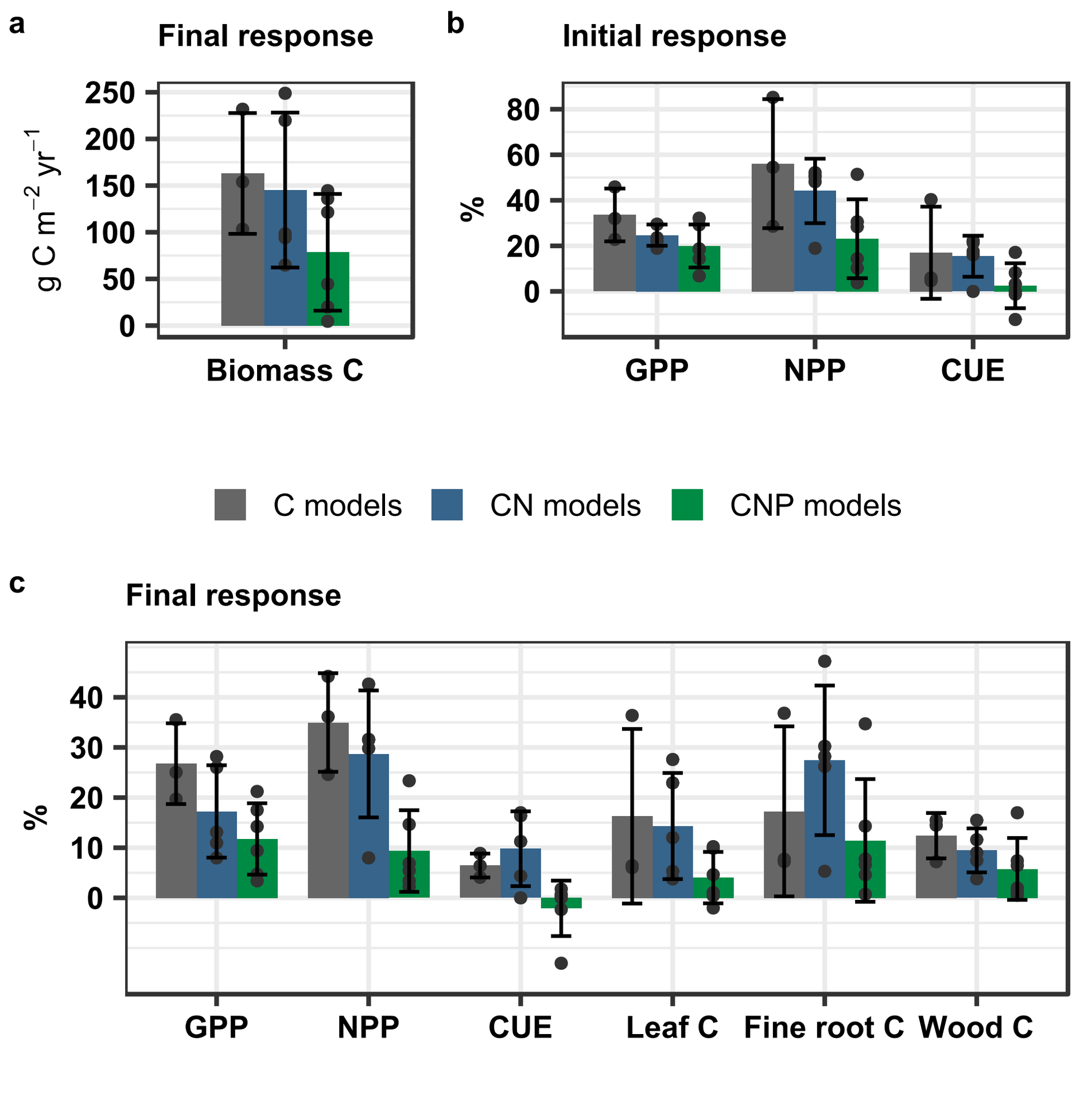
a
Final response
g C m^{-2} yr^{-1}
250
200
150
100
50
0
Biomass C
b
Initial response
%
80
60
40
20
0
GPP
NPP
CUE
C models
CN models
CNP models
c
Final response
%
40
30
20
10
0
GPP
NPP
CUE
Leaf C
Fine root C
Wood C

Control of phosphorus feedbacks on the biomass carbon response to eCO_2

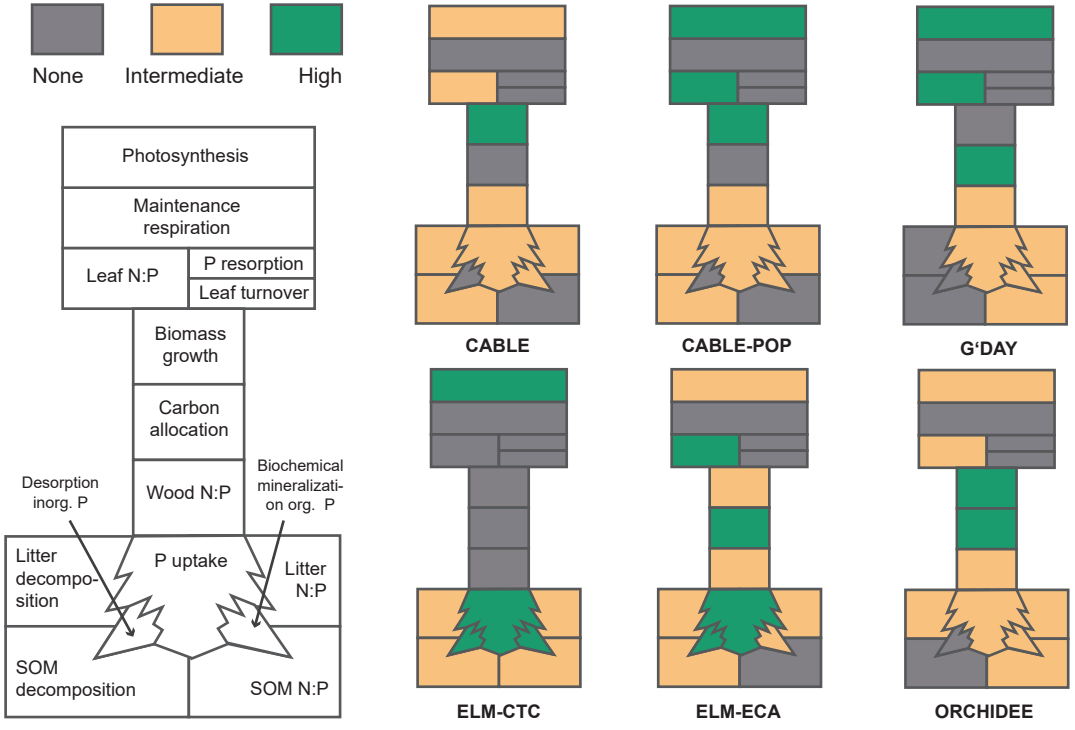

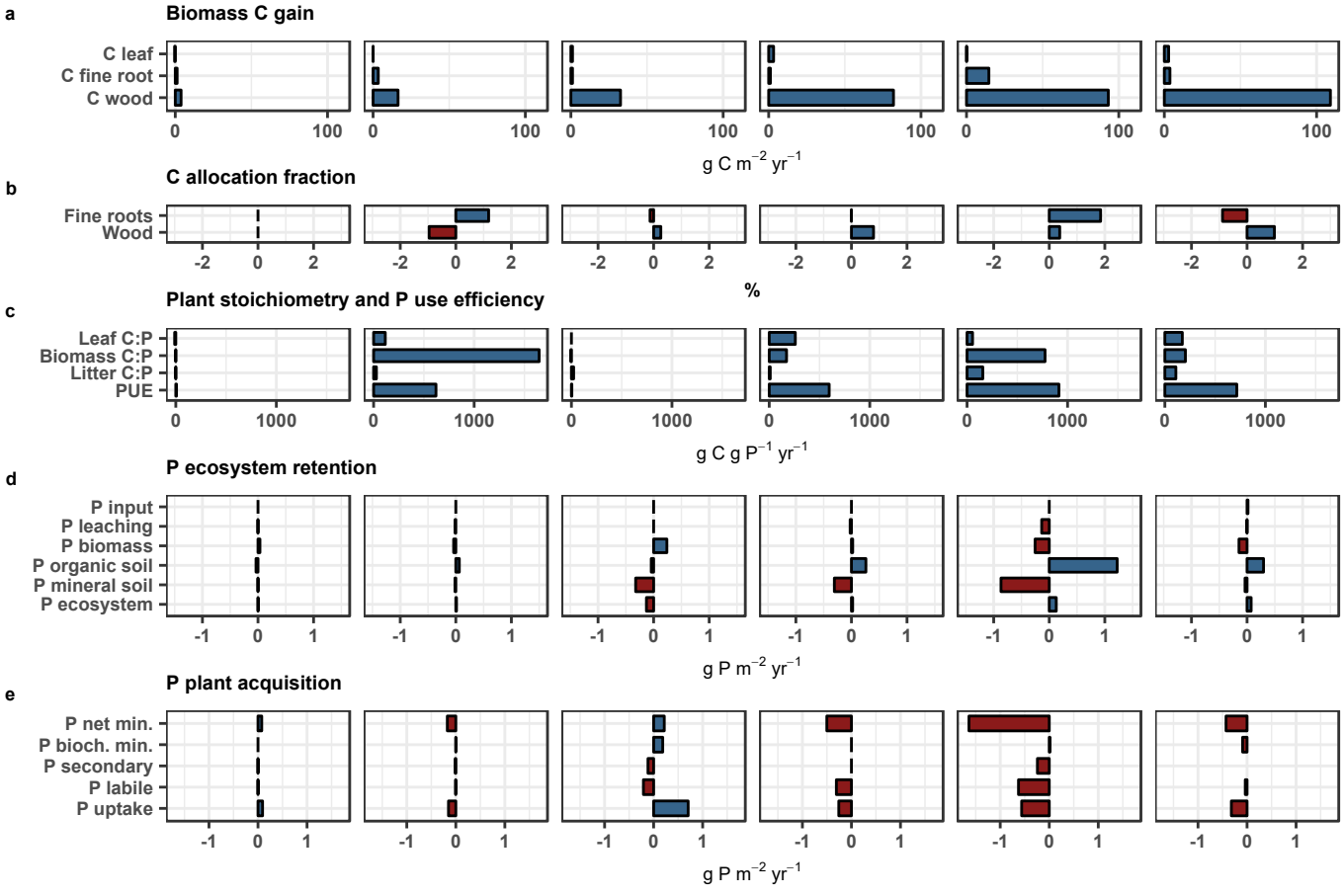
a
Biomass C gain
C leaf
C fine root
C wood
0
100
g C m−2 yr−1
b
C allocation fraction
Fine roots
Wood
-2
0
2
%
c
Plant stoichiometry and P use efficiency
Leaf C:P
Biomass C:P
Litter C:P
PUE
0
1000
g C g P−1 yr−1
d
P ecosystem retention
P input
P leaching
P biomass
P organic soil
P mineral soil
P ecosystem
-1
0
1
g P m−2 yr−1
e
P plant acquisition
P net min.
P bioch. min.
P secondary
P labile
P uptake
-1
0
1
g P m−2 yr−1